Chapter 1

FLUCTUATION CORRELATION SPECTROSCOPY IN CELLS:

Determination of molecular aggregation

E. Gratton[1], S. Breusegem[2], N. Barry[2], Q. Ruan[3], and J. Eid[4]

INTRODUCTION

Fluorescence Correlation Spectroscopy (FCS) was first introduced by Elson, Madge and Webb (1-5) for studying the binding process between ethydium bromide and DNA. When the ethydium dye binds to DNA its fluorescence quantum yield changes by a large factor. It is essentially not fluorescent when free in solution and it becomes strongly fluorescent when bound to double strand DNA. Although the processes are very different in nature, the instrumentation used for the FCS experiment is derived from dynamic light scattering. There are however major differences between dynamic light scattering and FCS. In the FCS experiment the fluorescence fluctuation arises because of the chemical reaction that changes the fluorescence properties of the dye and because the bound ethydium molecules could enter and leave the volume of excitation due to diffusion of the molecule. In dynamic light scattering the fluctuations arise from changes in the index of refraction due to local changes in the concentration of molecules. Therefore FCS is sensitive to all chemico-physical processes that could change the fluorescence intensity in a small volume. For the fluctuation in intensity to be measurable it is crucial that the volume of observation to be small so that only a few molecules are at any instant of time in the volume of observation.

The realization of small exaction volume was a major problem hindering the use of this technique and only recently, with the introduction of confocal microscopy and two-photon microscopy FCS the generation of sub-femtoliter volumes of observation has become a routine procedure. At nanomolar concentration a femtoliter volume contains

[1] Enrico Gratton, Laboratory for Fluorescence Dynamics, 1110 W. Green Street, University of Illinois at Urbana-Champaign, Urbana, IL 61801; [2] Sophia Breusegem, Nicholas Barry, University of Colorado Health Sciences Center, Denver, CO 80262; [3] Qiaoqiao Ruan, Abbott Laboratories, Abbott, IL 60064; [4] John Eid, Rowland Institute at Harvard, Cambridge, MA 02142

only few molecules. As a consequence of the Poisson distribution of the occupation number, the fluctuations in fluorescent intensity of a fluorescent dye in this small volume are appreciable. There are many methods to study chemical reactions and diffusion of molecules in solutions, but when it comes to the study of these reactions in cells, the problem becomes almost insoluble. The appeal of the FCS technique is that the confocal volume can be placed anywhere in the cell without disrupting the cell membrane of perturbing the cell. Therefore, as soon as two-photon microscopy was introduced by Denk, Strickler and Webb (6) we started to develop methods to study reactions in the cell interior using FCS in combination of two-photon fluorescence excitation (7,8). The necessary ingredients for FCS to work are methods to excite a small volume and very high sensitivity and dynamic range. The recent developments in microscopy, in new ultra-sensitive detectors and fast computers have made FCS a relatively simple to use technique. Commercial instruments are now available from several manufactures and the number of publications using the FCS technique is increasing very much.

Methods to produce a confocal or small volume

There are several possibilities for producing a relatively small volume for fluorescence excitation. These methods can be classified in two broad classes: methods that are limited by the wavelength of light and methods that are limited by construction of restricted volumes. Methods that are not limited by the wavelength of light are based on nanolithography, local field enhancements and near-field effects. Using these methods very small volumes can be achieved, on the order of 100 nm or smaller in size. However, these methods are not applicable to study the interior of cells. The methods commonly employed in cell studies are all limited by the wavelength of light and they are based on the following principles: confocal volume limited by the size of pinholes, multi-photon effects limited by the order of photon excitation, second harmonic generation, similar in volume to two photon excitation, stimulated emission and four-way mixing (Coherent Anti-Stokes Raman Scattering). In our lab, we have developed methods based on two-photon excitation. The excitation volume characteristic of two photon excitation has been approximated by a Gaussian-Lorentzian shape. The effective volume of excitation is about 0.1 fL, limited by the wavelength of the light used and by the numerical aperture of the objective. The point-spread-function (PSF) for one-photon excitation was modeled by the following expression (7):

$$I_{GL}(r,z) = I_0 \frac{2}{\pi} e^{-2\left(\frac{r^2}{w(z)^2}\right)} \left(\frac{w_0^2}{w(z)^2}\right)$$

where w(z) is related to the wavelength of the excitation source, λ, and the numerical aperture (NA) of the objective in the following manner:

$$w(z) = w_0\left(1+\left(\frac{z}{z_r}\right)^2\right)^{1/2}, \quad z_r = \frac{\pi w_0^2}{\lambda}, \text{ and } w_0 \approx \frac{1.22\lambda}{NA}.$$

w_0 is the diffraction limited $1/e^2$ beam waist (7).

Table 1. Orders of magnitude of number of molecules and diffusion time (for 1 μM solution, small molecule, water) in different volume of excitation.

Volume	Device	Size(μm)	Molecules	Time (s)
milliliter	cuvette	10000	$6x10^{14}$	10^{4}
microliter	plate well	1000	$6x10^{11}$	10^{2}
nanoliter	microfabrication	100	$6x10^{8}$	1
picoliter	typical cell	10	$6x10^{5}$	10^{-2}
femtoliter	confocal volume	1	$6x10^{2}$	10^{-4}
attoliter	nanofabrication	0.1	$6x10^{-1}$	10^{-6}

In Table 1, we report typical volumes that can be obtained using different techniques, the number of molecules in the volume (at a given bulk concentration) and the average time that a small molecule (in water at room temperature) will take to transit through that volume by random diffusion.

Advantages of two-photon excitation

There are several distinct advantages of the two-photon excitation method for the study of the cellular environment essentially due to the relatively low photo-toxicity of the near-ir radiation. Of course, the intrinsic two-photon excitation sectioning effects makes it possible to place the volume of illumination virtually everywhere in the cell body. For tissue work the penetration depth of two-photon excitation could be particularly useful. From the spectroscopic point of view, there is large separation between excitation and emission and virtually no second-order Raman effect. The high degree of polarization and the wavelength dependence of two-photon excitation which for several dyes extend over a large spectral region, can be exploited for specific applications based on light polarization.

FCS: time and amplitude analysis

In a typical fluctuation experiment a small volume is excited and the fluorescence from that volume is collected as a function of time. If the number of fluorescent molecules in that volume is not changing and if there are no chemical reactions that could change the quantum yield of the fluorescence, then the average number of the emitted photon is constant. However, the instantaneous number of photon detected is not constant due to the Poisson nature of the emission/detection process. This added shot-noise is independent of time. Instead, if the number of molecules in the excitation volume is changing or the quantum yield is changing, the fluorescence intensity will change with time which is characteristic of the processes that cause the change in the fluorescence intensity. For example, if the number of molecules change due to the diffusion of a molecule out of the excitation volume, the characteristic time of this process causes characteristic frequencies to appear in the fluorescence intensity recording. Furthermore, assume that we have four molecules in the excitation volume and one leaves, the relative change in intensity will be one-fourth. However, if we have 100 molecules in the excitation volume and one leaves, the relative change will be only 1/100. Therefore the ratio of the fluctuation to the average

signal is smaller the larger is the number of molecules in the volume. It can be shown that this ratio is exactly proportional to the inverse of the number of molecules in the volume of excitation (9). This relationship allows the measurements of the number of molecules in a given volume in the interior of cells (7).

A more interesting and common problem arises when molecules of different kind are simultaneously present in the same volume, either because of molecular heterogeneity or because of molecular reactions (10-12). One case of particular importance is when to macromolecules will come together to form a molecular aggregate. Let us assume that two identical proteins with one fluorescent probe each form a molecular dimer. This molecular species is different form the monomers because in carries twice the number of fluorescent moieties. When this aggregate enters the volume of excitation, it will cause a larger fluctuation of the intensity than a single monomer. Clearly, the amplitude of the fluctuation carries information on the brightness of the molecule.

On the basis of the previous discussion, the statistical analysis of fluctuations of the fluorescence signal must be done to recover the underlying molecular species and the dynamic processes that cause the change of the fluorescence intensity. It is customary to analysis the characteristic time of the fluctuation using the so called autocorrelation analysis. In this case, the autocorrelation function of the fluctuation intensity provides both the characteristic times of the system under exam and the number of fluorescent molecules in the excitation volume. In the case of identical molecules undergoing random diffusion in a Gaussian illuminated volume the characteristic autocorrelation function is given by the following expression (9):

$$G(\tau)=\frac{\gamma}{N}\left(1+\frac{8D\tau}{w_r^2}\right)^{-1}\left(1+\frac{8D\tau}{w_a^2}\right)^{-1/2}$$

where D is the diffusion constant, w_r and w_a are the beam waist in the radial and in the axial directions, respectively, N is the number of molecule in the volume of observation, γ a numerical factor that accounts for the non uniform illumination of the volume and τ the delay time. Other formulas have been derived for the Gaussian-Lorentzian illumination profile (7) and for molecules diffusing on a membrane (9).

The expression for the statistics of the amplitude fluctuations is generally given under the form of the histogram of the photon counts for a given sampling time Δt. This is known as the photon counting histogram (PCH) distribution. The analytical expression for the PCH distribution for a single molecular species of a given brightness has been derived for the 3D-Gaussian illumination profile (11) and is reported below.

$$p_{3DG}(k;V_0,\varepsilon)=\frac{1}{V_0}\frac{\pi\omega_o^2 z_0}{2k!}\int_0^\infty \gamma\left(k,\varepsilon e^{-4x^2}\right)dx \quad \text{, for } k>0$$

In this expression, V_o is the volume of illumination, ε is the brightness of the molecule and k is the number of photons in a give time interval. The integral, which contains the incomplete gamma function γ, can be numerically evaluated. Similar expressions have been derived for other shapes of the illumination volume (11). Before the development of the PCH, Qian and Elson (12) studied the effect of the intensity distribution using the

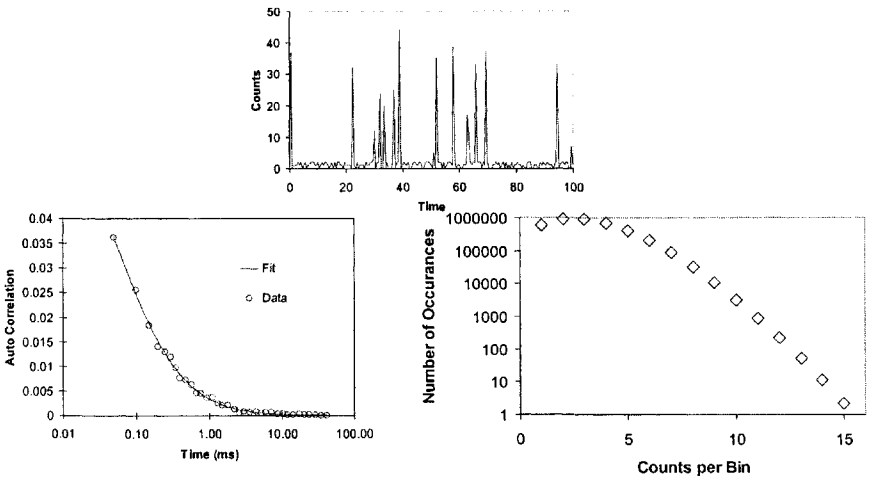

Figure 1. Upper panel: counts as a function of time. This is the original time trace data. Left panel: autocorrelation function of the time trace data from upper panel. Right panel: photon counting histogram of the time trace data in first panel.

so-called moment analysis distribution method.

A typical example of the time sequence of the fluorescence fluctuations and the calculation of the autocorrelation function and of the PCH distribution is shown in figure 1. The autocorrelation function provides the diffusion constant and the number of molecules N in the excitation volume. The PCH distribution provides the molecular brightness and the number of molecules also. In case of molecular aggregation, the autocorrelation function and the PCH distribution is fitted to a model for two or more species of different molecular brightness and of different diffusion constant (11). The particle size affects the autocorrelation function by shifting the autocorrelation curve to longer delay times for larger particle sizes. Figure 2 shows this effect for typical values of the diffusion constant of the GFP molecule (Green Fluorescent Protein) and fluorescein. The curve at smaller delay times is typical of a small molecule such as fluorescein in water (Diffusion constant of 300 $\mu m^2/s$). The next curve is typical of GFP in solution (Diffusion constant of 90 $\mu m^2/s$) and the curve on the lower panel is for a putative dimer of GFP (Diffusion constant of 70 $\mu m^2/s$). The difference between the monomer and the dimer is very small and difficult to detect in the presence of other factors, such as the changes in viscosity in the interior of cells.

For the PCH distribution, the effect of increasing the molecular brightness is that of shifting the curve to larger count number (figure 2, right panel). It is interesting to consider what happens if we mix two fluorophores of different brightness in the same sample. Theory predicts that we should obtain the convolution of the individual histograms rather than the sum. This is clearly shown in figure 3.

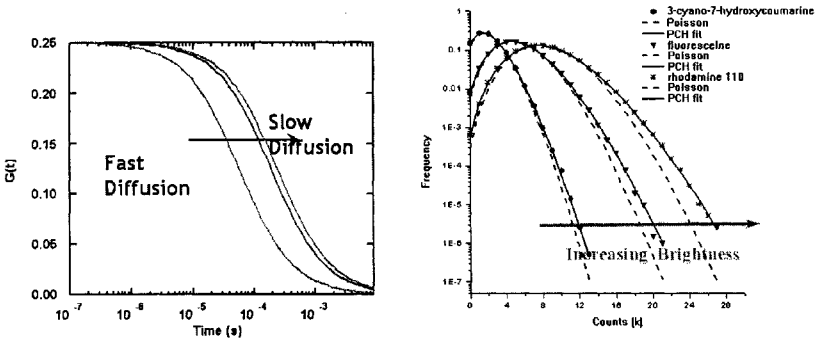

Figure 2. Left panel: Changes in position of the autocorrelation function as the value of the diffusion constant is decreased. The curve at the left is for fluorescein, the next curve is for GFP and the last curve is for a dimer of GFP molecules. Right panel: change in shape of the photon counting histogram as the brightness of the molecule is increased

The sum of the two histograms would have given two distinct distributions, but the experiments show that there is only one broad distribution which is the convolution of one PCH distribution with that of the other species. In this experiment, the molecules for sample 1 have a brightness of 5,600 counts/second per molecule (cpsm) and the concentration is about 1.08 molecules in the excitation volume as an average. For sample 2, the brightness is about 12,000 cpsm and the concentration is about 0.96 molecules in the excitation volume as an average. An equal volume of the two samples ware mixed together for the mixture sample.

The number occupancy fluctuations for each species in the mixture becomes a convolution of the individual specie histograms. The resulting histogram is then broader than expected for a single species.

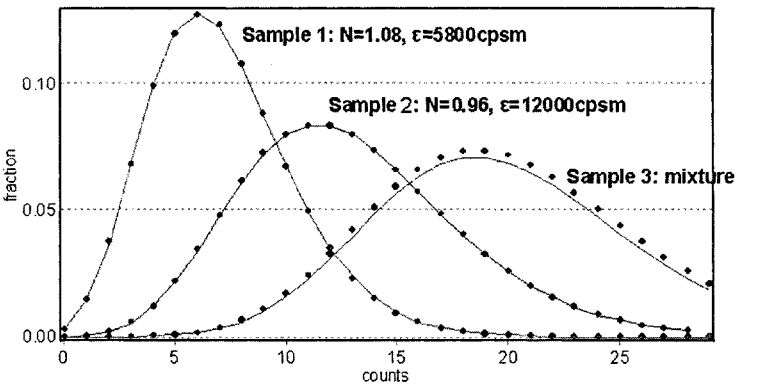

Figure 3. The convolution effect of adding two molecular species with different brightness. The mixture is not the sum of the two photon counting histograms but rather the convolution of the two distributions. N is the number of molecules in the excitation volume and e is the brightness of the molecules in units of counts/s per molecule.

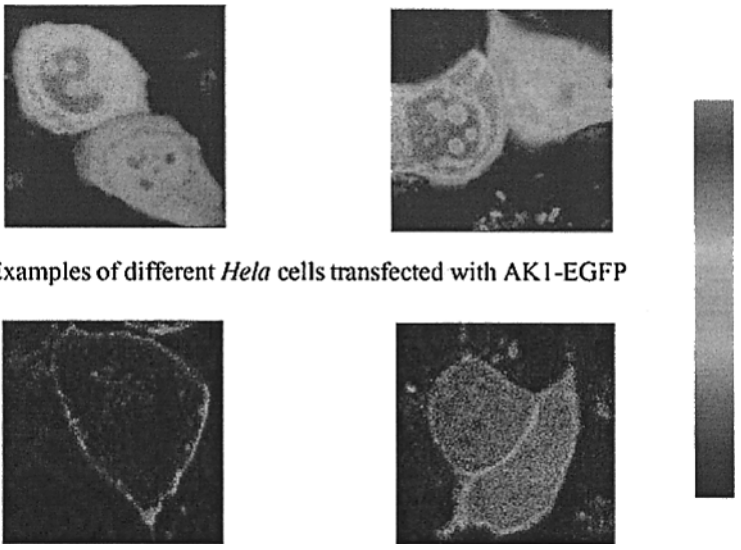

Figure 4. Cells expressing the ADK1-EGFP chimera protein (two upper panels) and cells expressing the ADK1β-EGFP chimera protein (lower panels).

Fluctuations in cells: Protein-membrane interactions

In this paragraph, we illustrate the application of the FCS technique for the determination of the diffusion constant of EGFP (Enhanced GFP) and EGFP constructs in cells. Hela cells were transfected to produce the EGFP protein and a construct of EGFP with two different variants of the adenylate kinase protein as described in Ruan et al. (13). As the images figure 4 show, the EGFP-ADK1 protein is distributed everywhere in the cell, while the construct of adenylate kinase EGFP-ADK1β is preferentially located on the membrane of the cells.

In figure 5, the autocorrelation curve to the left is for the EGFP protein in solution. The diffusion constant corresponding to this curve is 90 $\mu m^2/s$. This value corresponds exactly to what should be expected given the molecular weight of the protein and the viscosity and temperature of the experiment (14). The next curve toward the right at longer delay times corresponds to the same protein but in the cytoplasm of the Hela cells. The value of the diffusion constant is now strongly decreased, presumably due to the larger viscosity of the cytoplasm. The next two curves, almost superimposed, correspond to the two constructs of EGFP with ADK1 and ADK1β. The two proteins are identical except for the addition of a 18-aminoacid peptide for the ADK1β protein. These proteins diffuse in the cytoplasm with an apparent diffusion constant of about 13 $\mu m^2/s$.

If we focus the laser beam on the cell membrane, the autocorrelation function shape

changes dramatically. The form of the autocorrelation function is typical of that of two diffusing components as shown in figure 6, above. If the laser beam is focused in different points in the cytoplasm of the same cell, we obtain a series of values of the diffusion constant which are different in different position in the cell (figure 7). This study demonstrates that the interior of the cell is highly heterogeneous from the point of view of the diffusion of protein molecules. The heterogeneity of the diffusion could be due to interactions of the protein with other cellular components which results in slowing the motion of the protein.

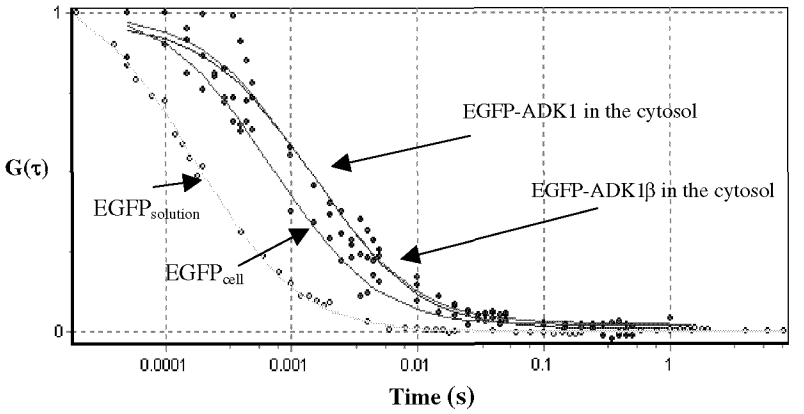

Figure 5. Autocorrelation curves for EGFP in solution and in the cytoplasm of Hela cells (two left curves) and for the chimera protein EGFP-ADK1 and EGFP-ADK1β (two right curves).

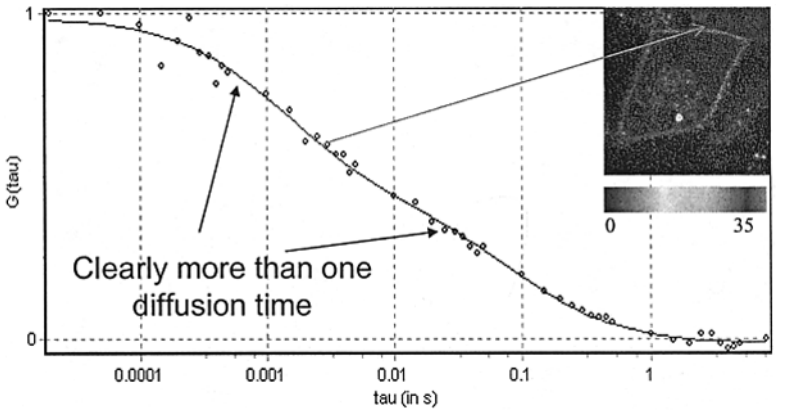

Figure 6. Autocorrelation curve for EGFP-ADK1β when excitation volume is placed on the plasma membrane. Two diffusion constants are clearly distinguished with values of 13 and 0.18 m^2/s.

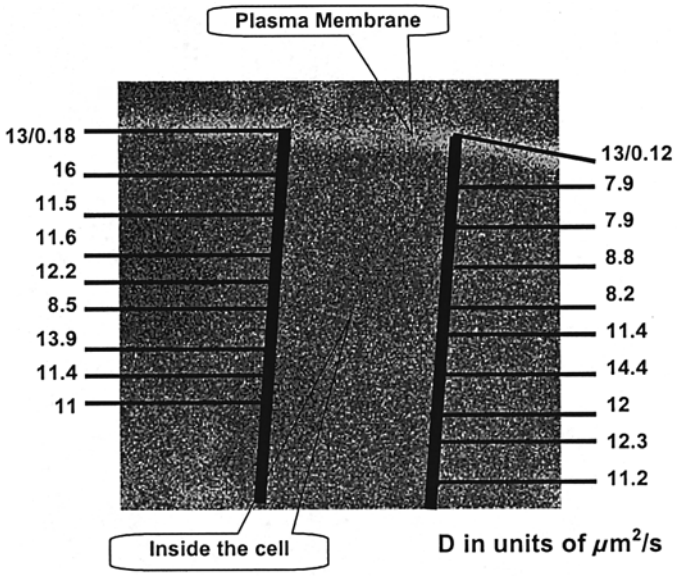

Figure 7. Values of the diffusion constants obtained in different points in the cell. The values in units of m^2/s are given. When the measurement is done in the region of the cytoplasmatic membrane, two characteristic values for the diffusion constant are obtained and reported.

Cross-correlation methods

Until now, we have considered fluorescent molecules of the same color and same intensity. If there are two molecular species that differ by color and/or intensity, it is possible to detect the emission using two independent detectors that are sensitive to the two different colors. Then, the statistical analysis can be done taking into account the correlation of the fluctuations in the two detector channels. This technique is called cross-correlation (15). Fluctuation cross-correlation can provide information that is not attainable using a single detection channel. The statistical analysis is performed along similar lines as already described for one channel detection. In the dual channel experiment, we calculate the cross-correlation between the signals from the two channels and we can also construct two-dimensional photon counting histograms. In this presentation, we are only discussing the cross-correlation function and one application for the detection of internal protein dynamics. The following expression mathematically defines the cross-correlation function between two signals F1 and F2 which vary as a function of time.

$$G_{ij}(\tau) = \frac{\langle dF_i(t) \cdot dF_j(t+\tau) \rangle}{\langle F_i(t) \rangle \cdot \langle F_j(t) \rangle}$$

Let us consider the situation shown in figure 8, in which we have two kinds of

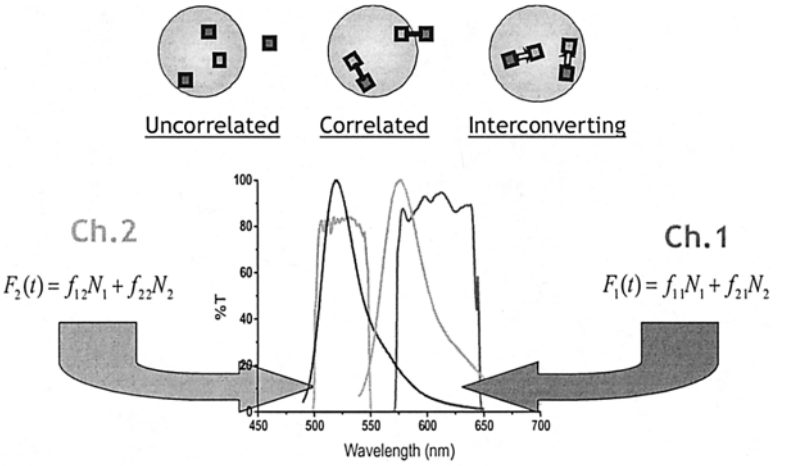

$$G_{12}(0) \propto \left[\frac{f_{11}f_{12}\langle N_1 \rangle + f_{21}f_{22}\langle N_2 \rangle}{f_{11}f_{12}\langle N_1 \rangle^2 + (f_{11}f_{22} + f_{21}f_{12})\langle N_1 \rangle \langle N_2 \rangle + f_{21}f_{22}\langle N_2 \rangle^2} \right]$$

Figure 8. Upper panel: schematic representation of different possibilities of molecular species which are uncorrelated, correlated and inter-converting. Middle panel: Spectral cross-talk for the specific filters used in the experiments described in this contribution. Lower panel: The cross-correlation G(0) term for the case in which there is cross-talk between the two channels.

molecular species. If the molecular species are uncorrelated, the common (to the two channels) fluctuation on the average will reduce to zero. Therefore, if the cross-correlation is zero, we can conclude that the molecular species are independent.

If the two molecular species are connected one to the other, every time the intensity in one channel changes, it will also change in the other channel. The two signals will be fully correlated. There is a third important situation in which one molecular species changes into the other. This physical process will give rise to an anti-correlation between the signal from the two channels since when one signal increases the other will decrease and *vice versa*.

The cross-correlation at delay time zero $G_{12}(0)$ depends only on the relative contributions of the two species on the two channels. This quantity depends on the relative brightness and number of molecules present in the volume of excitation as shown in the formula in figure 8, above.

This formula is important because it shows that even if there is no physical correlation between two molecules, they could appear to be correlated because of the non-perfect separation of the fluorescence of one molecule from the other. In most practical situations it is impossible to completely separate the emission of one molecule from the other since the red tail of the emission of the bluer molecule inevitably superimpose with the emission of the redder molecule. However this effect can be accounted for by measuring the spectral cross-talk between the two channels.

Cross-correlation and Molecular Dynamics

To demonstrate that the cross-correlation measurement can provide information on internal protein dynamics we studied the cameleon protein. The cameleon protein that was used is a fusion protein consisting of calmodulin and the calmodulin binding peptide M13 sandwiched between cyan fluorescent protein (CFP) and yellow fluorescent protein (YFP). This protein was first constructed by Miyawaki et al. (16) as schematically shown in figure 9. In the presence of Ca^{2+} the CaM bends in such a way as to position the GFP constructs closer together allowing for an increase in the FRET (Förster Resonance Energy Transfer) efficiency (figure 9, right panel). FRET occurs between the CFP and the YFP when their distance became smaller than the characteristic FRET distance. Since the CaM protein is more compact when calcium is bound, this state has large FRET efficiency. To switch the cameleon into the low FRET efficiency conformation 30 mM EDTA was added (figure 9, right panel) to remove the calcium.

The important question we want to answer in this experiment is whether or not the FRET efficiency changes with time due to internal protein dynamics. The FRET efficiency is a function of the relative distance between the donor and the acceptor as well as of their relative orientation. If the FRET efficiency changes, then the spectrum will shift from blue to yellow and *vice versa*. We predict that the typical signature of the anti-correlation due to species inter-conversion between the two channels should be visible if there are dynamics changes in the FRET efficiency during the time the molecules transit across the excitation beam. This effect is shown schematically in figure 10A.

The donor autocorrelation exhibits the expected extra relaxation under the calcium saturated conditions (figure 10B, bottom). After the addition of calcium, the cross-correlation curve contains the anticipated anti-correlation (figure 10B, bottom) although it is less pronounced than in figure 10B, top, where the expected curve for this process has been simulated. This is likely a result of a large fraction of non-switching particles. Nonetheless, the anti-correlation effect is clearly visible. After the addition of dynamics yields a very small contribution of the relaxation part, indicating that

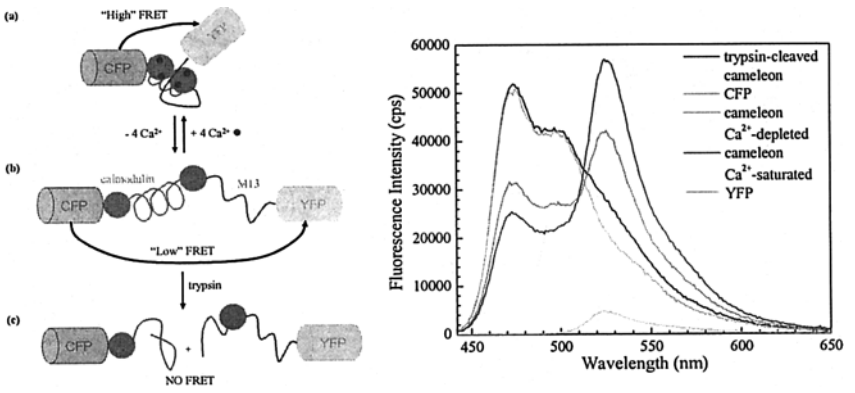

Figure 9. Left panel: schematic of the close or high FRET state in the presence of calcium and of the extended low FRET state in the absence of calcium. Right: different spectra obtained from the trypsin cleaved cameleon protein and the limiting spectra at high and low calcium concentration.

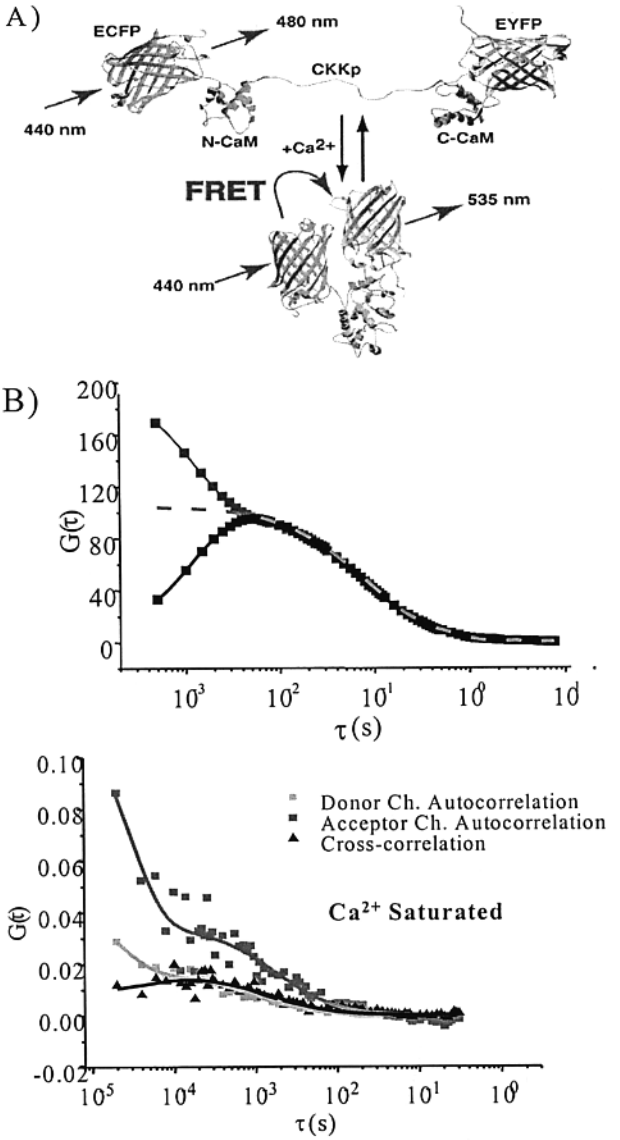

Figure 10. Top panel (A) shows the high FRET close conformation and the low FRET open conformation. Panel B, middle graph, shows the expected effect on the autocorrelation and cross correlation curves if the opening and closing reaction occurs with a characteristic relaxation time of 20 microseconds. The bottom graph shows experimental data for the auto and cross-correlation. The cross-correlation shows the characteristic anti-correlated behavior. The characteristic inter-conversion time was 20 microseconds.

a pure diffusion fit is adequate to describe the data. When calcium is added, this relaxation component increases. The curve at low calcium concentration is also much noisier than the one obtained under the calcium saturated condition. The acceptor autocorrelation curve exhibits the extra relaxation for the calcium saturated condition and cannot be fit even to pure diffusion when the EDTA is added (figure 10B, top). This is because after the EDTA is added the FRET efficiency drops to zero percent and since there is no appreciable direct excitation of YFP, the entire signal is lost.

This effect due to the protein dynamics could be exploited to determine the concentration of calcium in the cell. Of course, this protein has been engineered to have spectral sensitivity to calcium. However, for the study of the interior of cells, this relaxation behavior could also be sensitive to calcium concentration. The relaxation behavior is also present in the autocorrelation curve, showing that single channel measurements could be enough for the determination of calcium concentration.

Conclusions

We have shown that the statistical analysis of fluctuations of the fluorescence signal is a powerful tool for the study of chemical reactions both in solutions and in the interior of cells. The crucial requirement for the success of the fluctuation experiments is a means to confine the excitation of the fluorescence to a small volume, on the order of a fraction of a femtoliter. This confinement of the excitation can be achieved using confocal pinholes or two-photon excitation methods. Two-photon excitation is particularly benign to cells since out of focus photo bleaching is avoided. For solution studies, this advantage is less important. The study of the reactions in the cell interior has become a very active field of research. The dynamics of the cell interior is fundamental for life. Optical methods, in particular the far-field methods described in this presentation, provide a non-invasive way to observe the cell in action with minimal perturbation. The cross-correlation experiments described in this work for the measurement of internal protein fluctuations are also unique because they provide a relatively simple method to access the time range in the microsecond time scale which is very difficult to obtain using rapid mixing. Cross-correlation provides information on internal dynamics in the microsecond to millisecond range and it is applicable to the interior of cells. Two-photon excitation simplifies problems associated with color aberration since a single excitation wavelength can be used to excite different fluorophores.

Acknowledgements

This work was performed using the instrumentation of the Laboratory for Fluorescence Dynamics, a national research resource funded by the National Institutes of Health, NCRR, grant PHS 5 P41 RR03155 and the University of Illinois.

References

1. Elson, E.L. and Magde, D. 1974. Fluorescence correlation spectroscopy. I. *Conceptual Basis and Theory. Biopolymers.* 13:1-27.

2. Magde, D. 1976. Chemical kinetics and fluorescence correlation spectroscopy. *Q. Rev. Biophys.* **9**:35-47.
3. Magde, D., Elson E. and Webb, W.W. 1972. Thermodynamic fluctuations in a reacting system: Measurement by fluorescence correlation spectroscopy. *Phys. Rev. Lett.* **29**:705-708.
4. Magde, D., Elson, E.L. and Webb, W.W. 1974. Fluorescence correlation spectroscopy. II. An experimental realization. *Biopolymers.* **13**:29-61.
5. Magde, D., Webb, W.W. and Elson, E.L. 1978. Fluorescence correlation spectroscopy. III. Uniform translation and laminar flow. *Biopolymers.* **17**:361-376.
6. Denk, W., Strickler, J.H. and Webb, W.W. 1990. Two-photon laser scanning fluorescence microscopy. *Science.* **248**:73-76.
7. Berland, K.M. 1995. *Two-photon fluctuation correlation spectroscopy: method and applications to protein aggregation and intracellular diffusion.* University of Illinois at Urbana-Champaign, Urbana.
8. Berland, K.M., So, P.T.C., and Gratton, E. 1995. Two-photon fluorescence correlation spectroscopy: Method and application to the intracellular environment. *Biophys. J* **68**:694-701.
9. Thompson, N.L. 1991. Fluorescence correlation spectroscopy. In *Topics in Fluorescence Spectroscopy.* Lakowicz, J.R. (ed.), Plenum, NY 337-378.
10. Palmer, A.G. and Thompson, N.L. 1987. Molecular aggregation characterized by high order autocorrelation in fluorescence correlation spectroscopy. *Biophys J* **52**:257-270.
11. Chen, Y., Muller, J.D., So, P.T. and Gratton, E. 1999. The photon counting histogram in fluorescence fluctuation spectroscopy. *Biophys J.* **77**(1):553-567.
12. Qian, H. and Elson, E.L. 1990. Distribution of molecular aggregation by analysis of fluctuation moments. *Proc Natl. Acad. Sci. U S A.* **87**:5479-5483.
13. Ruan, Q., Chen, Y., Gratton, E., Glaser, M. and Mantulin, W.W. 2002. Cellular characterization of adenylate kinase and its isoform: two-photon excitation fluorescence imaging and fluorescence correlation spectroscopy. *Biophys J* **83**(6):3177-3187.
14. Chen, Y., Muller, J.D., Ruan, Q., Gratton, E. 2002. Molecular brightness characterization of EGFP *in vivo* by fluorescence fluctuation spectroscopy. *Biophys J* **82**(1):133-44.
15. Schwille P, Meyer-Almes, F. J. and Rigler, R. 1997. Dual-color fluorescence cross-correlation spectroscopy for multicomponent diffusional analysis in solution. *Biophys J* **72**: 1878-1886
16. Miyawaki, A., Llopis, J., Heim, R., McCaffery, J. M., Adams, J. A., Ikura, M. and Tsien, R. Y. 1997. Fluorescent indicators for Ca2+ based on green fluorescent proteins and calmodulin. *Nature (London)* **388**, 882-887.